

On the properties of superconducting planar resonators at mK temperatures

T. Lindström,* J.E. Healey, M.S. Colclough, and C.M. Muirhead
University of Birmingham, Edgbaston, Birmingham B15 2TT, UK[†]

A.Ya.Tzalenchuk
National Physical Laboratory, Hampton Road, Teddington, TW11 0LW, UK
 (Dated: November 3, 2019)

Planar superconducting resonators are now being increasingly used at mK temperatures in a number of novel applications. They are also interesting devices in their own right since they allow us to probe the properties of both the superconductor and its environment. We have experimentally investigated three types of niobium resonators - including a lumped element design - fabricated on sapphire and SiO₂/Si substrates. They all exhibit a non-trivial temperature dependence of their centre frequency and quality factor. Our results shed new light on the interaction between the electromagnetic waves in the resonator and two-level fluctuators in the substrate.

I. INTRODUCTION

The superconducting microwave resonator is an ubiquitous device with uses ranging from the very practical - such as filters for telecommunications - to rather exotic such as tests of cavity quantum electrodynamics. Over recent years there has been a resurgence in the interest in on-chip resonators; the primary reason being their use as very sensitive radiation detectors in e.g. astronomy and much of the work to date has been motivated by the need to understand noise properties of kinetic inductance detectors (KID)^{1,2,3}. Resonators are also being used as elements in circuitry for quantum information processing⁴. The latter has triggered a wave of investigations into the properties of resonators when operated at mK temperatures and very low (ideally single photon) microwave powers. Of particular interest has been the effects of two-level fluctuators (see e.g.^{5,6} and references therein). Superconducting resonators at microwave frequencies differ from that of their normal metal counterpart primarily because of their high quality factor (Q) and a relatively large kinetic inductance. For example, for an ideal high- Q LC resonator we can write the centre frequency as $f_0 = (2\pi\sqrt{(L + L_K)C})^{-1}$ where L_K is the contribution from the kinetic inductance. L_K depends on the order parameter and therefore varies with temperature, but can also be altered e.g. by a weak magnetic field⁷. As the temperature goes down the centre frequency increases monotonically while the conductor losses decrease (leading to a higher quality factor), as described by the Mattis-Bardeen theory⁸. However, at temperatures $\sim T_c/10$, these mechanisms saturate (in Nb and its compounds around 1 K) and other effects become prominent^{1,3,7}, most notably a *decrease* in the centre frequency as the temperature is reduced. This 'back-bending' is now widely believed to be due to the presence of two-level fluctuators (TLF) in the substrate.

Here we will discuss measurements of the centre frequency and losses in three types of Nb resonators: conventional $\lambda/2$ and $\lambda/4$ geometric resonators and a recently developed type of lumped element resonator⁹.

II. THEORY

A generic expression for the transmittance, S_{21} of a transmission line shunted by a resonator (e.g. the lumped element and $\lambda/4$ resonators considered here) can be written

$S_{21} = 2 \left[2 + \frac{g}{1+2jQ_u\delta f} \right]^{-1}$ where Q_u is the unloaded quality factor (Q in the absence of coupling to the feed-line), g is a coupling parameter $\propto Q_u$ - the exact expression for which will depend on the type of resonator used- and $\delta f = (f - f_0)/f_0$ is the fractional shift from resonance. The value of Q_u is in general given by summing over all loss mechanisms $\sum_k Q_k^{-1}$ but losses in the dielectric and the superconducting film itself¹⁰ usually dominate in planar resonators and radiation losses etc. can be neglected.

At sub-Kelvin temperatures one would expect the properties of a dielectric to stay essentially constant. However, experimentally one finds a variation in both the effective dielectric constant and losses. Much of this can be explained if one assumes the presence of a bath of TLF that couple to the resonator via their electric dipole moment. Many of the details of the corresponding theory were worked out over 30 years ago when the effects of TLF in glasses at low temperatures were being investigated¹¹. The theory is based on the application of the Bloch equations to an ensemble of spin systems and while it is simple is nevertheless captures most of the essential physics. For resonant absorption due to an ensemble of TLF the absorption α has the form^{12,13}

$$\alpha = \frac{\pi\omega nd^2}{3c_0\epsilon_0\epsilon_r} \left(1 + \frac{P}{P_c} \right)^{-1/2} \tanh \left(\frac{\hbar\omega}{2k_B T} \right) \quad (1)$$

where ω is the measurement frequency, d is the dipole moment, c_0 is the speed of light in vacuum and n is the density of states of the TLF that couple to the stray field of the resonator. Note that this density should in principle depend on frequency, but is experimentally often found to be constant. The temperature dependence of the absorption reflects the population difference of the two states of the fluctuators, as the temperature increases

the TLF will therefore absorb *less* power. Note that Eq. 1 only accounts for *resonant* absorption, non-resonant relaxation processes due the TLF bath are not taken into account.

The relation above predicts a power dependence of the absorption $\propto P^{-1/2}$ above some critical power P_c , although in practice one may reasonably expect another high-power roll-off once all the TLF are saturated and (non-resonant) relaxation starts to dominate (a process known in optics as *bleaching*). The critical intensity is given by $P_c = 3\hbar^2 c_0 \epsilon_0 \epsilon_r / 2d^2 T_1 T_2$ where T_1 and T_2 are the relaxation and the dephasing times of the TLF, respectively.

The variation in permittivity is dominated by resonant processes and can therefore be found by applying the Kramer-Kronig relations to Eq.1

$$\frac{\epsilon(T) - \epsilon(T_0)}{\epsilon(T_0)} = -\frac{2nd^2}{3\epsilon} \left[\ln \left(\frac{T}{T_0} \right) - (g(T, \omega) - g(T_0, \omega)) \right] \quad (2)$$

where $g(T, \omega) = \text{Re}\Psi(\frac{1}{2} + \hbar\omega/2\pi i k_B T)$, T_0 is a reference temperature and Ψ the complex digamma function significant only for $kT \lesssim \hbar\omega/2$. From cavity perturbation theory we then have that $\Delta f_0/f_0 = -F/2\Delta\epsilon/\epsilon$, F being a filling factor which depends on the geometry and the electric field distribution. The substrate filling factor varies slightly between the three types of resonator discussed here; but is over 0.9 in all cases. For samples on SiO₂/Si substrates the contribution of the SiO₂ layer to F is about 0.2. Eq. 1 predicts an upward turn in the temperature dependence of the centre frequency at mK temperatures, where the $g(T, \omega)$ term is important. In the experiments by Gao *et al*¹⁴ Eq. 2 was used to fit the temperature dependence of the resonance frequency, but the low-temperature upturn was not clearly observed.

The aim of this experimental study is to verify whether the theory developed for a spin solution in glass can accurately describe the temperature and power dependence of the resonance frequency and losses in superconducting resonators at mK temperatures.

III. EXPERIMENTAL

We have fabricated a wide variety of $\lambda/2$, $\lambda/4$ and lumped element (LE) niobium resonators (see fig. 1) on R-cut sapphire and thermally oxidized high-resistivity ($> 1 \text{ k}\Omega/\text{cm}^2$) silicon substrates with 400 nm of SiO₂. The simplest design is the in-line $\lambda/2$ resonator. Its advantages is that it can be made with loaded quality factors of $> 10^6$ and is easy to measure (due to the high S/N ratio on resonance), there is however only one resonator per chip and a calibrated measurement is needed in order to quantify its unloaded quality factor (which is difficult at mK temperatures). $\lambda/4$ resonators have the advantage that their parameters can be extracted relatively easily (using numerical fitting) from an uncalibrated measurements since the transmittance far from resonance can

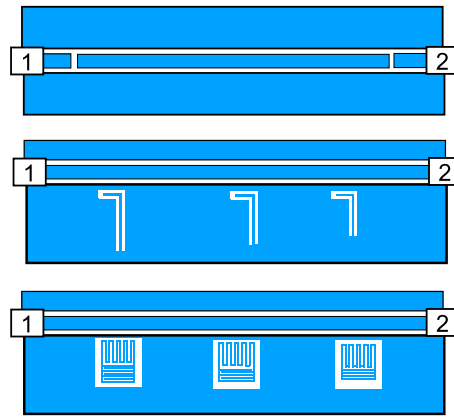


FIG. 1: Illustration (*not to scale*) showing the geometry and measurement configuration (ports $2 \rightarrow 1$) for the three types of resonators used in this work. From top to bottom: $\lambda/2$, $\lambda/4$ and Lumped element (LE) resonator.

be used as a reference level. It is also possible to couple many $\lambda/4$ resonators to a common feedline, making it possible to measure in a frequency-multiplexed configuration. The lumped element resonator shares these advantages and is much more compact (typical size is about $200 \times 200 \mu\text{m}^2$) than geometric resonators. Our LE resonators fabricated in Nb on sapphire exhibit loaded Q of about $1 \cdot 10^5$ with an unloaded Q that is about 3 times higher; i.e the resonators are by design overcoupled.

The structures were patterned in 200 nm thick sputtered Nb films using ion-beam etching and were designed to have a their centre frequencies in the c-band (4-8 GHz). Table I shows a summary of the samples discussed in this paper. Other resonators measured to-date showed similar behaviour. Each chip is $5 \times 10 \text{ mm}^2$ in size and incorporates a central 50Ω coplanar feed-line and one or more resonators. For the measurement the chip is glued to a gold-plated alumina carrier inside a superconducting box. All measurements (with the exception for the data above 1 K in fig. 4) were carried out in a dilution refrigerator with heavily filtered microwave lines. The transmitted

TABLE I: Summary of the resonators used in these experiments presented in this paper

	Type	Chip	Substrate	f_0 at 50 mK (MHz)
R1	$\lambda/2^a$	A	SiO ₂ /Si	6037
R2	$\lambda/4$	B	SiO ₂ /Si	5040
R3	$\lambda/4$	B	SiO ₂ /Si	5795
R4	$\lambda/4$	B	SiO ₂ /Si	8100
R5	LE	C	SiO ₂ /Si	6805
R6	LE	C	SiO ₂ /Si	7250
R7	LE	C	SiO ₂ /Si	7813
R8	LE	D	Sapphire	6046
R9	LE	D	Sapphire	6458
R10	LE	D	Sapphire	6959

^aSingle resonator on the chip, measured in-line

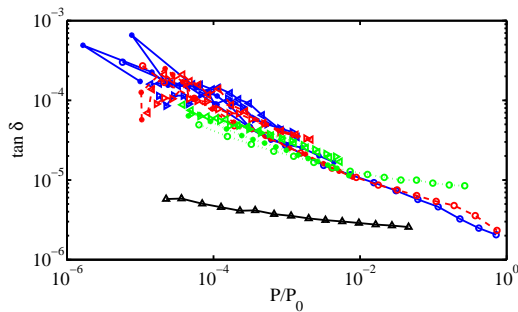


FIG. 2: Loss tangent for 3 lumped element resonators (R5-R7: green dotted, red dashed and solid blue line, respectively) on SiO₂/Si at 4 different temperatures: 50mK(○), 100mK (*), 250mK(▲) and 340mK(■). The lowest curve (▲) shows a similar measurement at 30mK for R8, a resonator on sapphire. All curves were measured using the same *applied* power.

signal was amplified using an InP HEMT amplifier held at 1 K with a noise temperature of about 4 K, before further amplification stages at room temperature.

IV. RESULTS

Figure 2 show how the loss tangent $\tan \delta = 1/Q_u \propto \alpha$ depends on the power entering the resonator $P = 2Q_u/\omega(1 - S_{21})S_{21}P_{in}$ for three different lumped element resonators on SiO₂/Si coupled to the same on-chip transmission line and measured simultaneously. Absolute power metrology at mK temperatures is unfortunately very problematic so only relative measurements were possible. However, we estimate that the maximum power reaching the chip during the measurements is about -70 dBm, meaning P_0 is of the order of 10^{-16} W. Shown is also R8, a sapphire resonator of the same design. For the resonators fabricated on SiO₂/Si the curves have a slope of approximately -0.4 in this range of applied powers. Eq. 1 predicts dielectric losses changing with a slope of -0.5 for powers above P_c and power-independent behavior below P_c , it is therefore possible that we are in the intermediate regime. However, it is also possible that losses in the superconductor not captured by Eq. 1 play a role. Indeed the current distribution in superconducting resonators is such that its *local* value can be significant even at our lowest microwave powers leading to higher conductor losses as the power is increased. The overall effect would be again a smaller slope. It is interesting to note that the power entering the resonator depends on Q and Q also -due to the TLF- in turn depends on the power. Hence, the system is non-linear and in principle weakly hysteretic.

The main conclusion from fig. 2 is that the loss tangent is strongly power dependent for SiO₂/Si whereas a weaker dependence is observed for identical structures on sapphire; Q only changes by about a factor of two even when the power is changed by over 40 dB.

Experimentally, the temperature dependence of the resonance frequency of superconducting resonators is quite complicated since it is affected both by the properties of the superconducting film (e.g. the kinetic inductance) and changes in the dielectric and it is in general difficult to separate these two effects. However, at temperatures $\ll T_c$, which is the case here, we can assume that the thermal effects on the kinetic inductance are small. Figure 3 shows the relative shift of the resonance frequency as a function of the normalized temperature $\hbar\omega/k_B T$ together with a fit to Eq. 2. All data from the resonators on SiO₂/Si can be fitted using a single parameter; we find $Fd^2n/3\epsilon = 6x10^{-5}$ and $2.8x10^{-6}$ for the SiO₂/Si and sapphire respectively; a difference of about a factor of twenty; consistent with the loss tangent measurements. Note that the curves shown come from several resonators of two different designs (on two separate chips), with each resonator measured at several different power levels, but they they can all be fitted using a single fitting parameter.

In order to verify that the temperature dependence does not depend on the geometry or our data analysis, we have in addition to lumped-element and $\lambda/4$ (in shunt configuration) resonators also measured in-line $\lambda/2$ coplanar resonators. While it is difficult to extract parameters such as the coupling strength and unloaded quality factor they have the advantage that one can measure very undercoupled resonators as is the case here. Fig. 4 shows the measured temperature dependence of $1/Q_l$ and f_0 for a $\lambda/2$ resonator. Again we can fit all the f_0 curves using a single parameter, although in this case the fitting parameter $Fd^2n/3\epsilon$ is $4.95x10^{-5}$, slightly

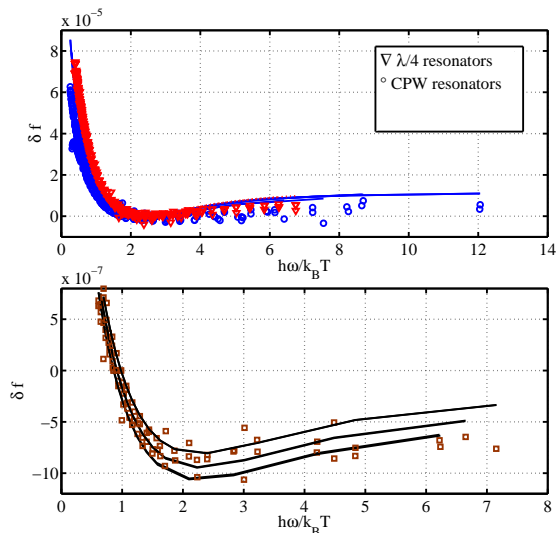


FIG. 3: Frequency shift as a function of the normalized frequency for LE resonators R2 to R7 on SiO₂/Si (*top*); and R8 to R10 sapphire(*bottom*). The solid lines show fits to theory. The log term dominates at small $\hbar\omega/k_B T$ whereas $g(t)$ becomes important in the opposite regime.

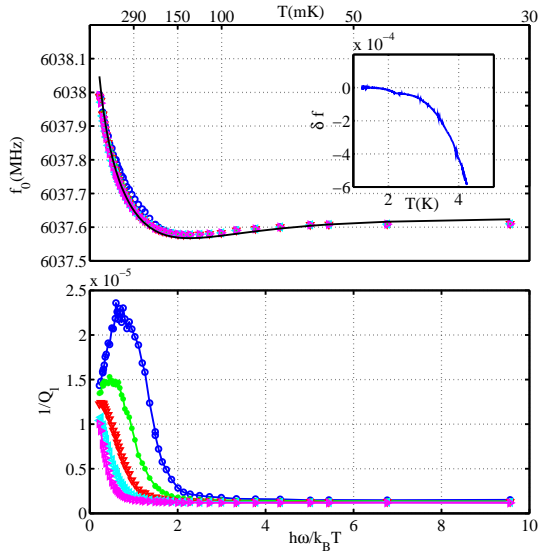


FIG. 4: Centre frequency (*Top*) and $1/Q_l$ (*Bottom*) at five different powers and as a function of temperature for sample R1, a $\lambda/2$ resonator fabricated on SiO_2/Si . Each successive curve (top to bottom) corresponds to an increase in power by 2 dB. *Inset*: $\lambda/2$ resonator measured above 1K where the behavior follows the Mattis-Bardeen theory.

lower than for the other samples. Some of this difference is likely to be due to somewhat different filling factors. We note that the values for $Fd^2n/3\epsilon$ we obtain from samples fabricated on sapphire results are consistently lower than those reported by Gao *et al.* Shown is also a separate measurement up to 4K. In this interval the dependence is dominated by the changing kinetic inductance and is well described by the Mattis-Bardeen theory.

Eq.(1) gives the correct power dependence of losses and temperature dependence of resonance frequency. On the other hand, the experimental temperature dependence of the losses $1/Q_l$ (Q_l is the loaded quality factor) does not follow the theoretical temperature dependence Eq. 1, which is only valid for *resonant* absorption. One explanation might be that the relative significance of *relaxation* (non-resonant) absorption processes increases for temperatures below $\approx k_B T$. As the power is increased, resonant losses are generally suppressed and the relaxation mechanism becomes important at increasingly high temperatures - the peak in absorption shifts as $\Delta T \propto P^{-3/2}$.

A practical point to note is that losses in the crossover regime $\hbar\omega \approx k_B T$ are very sensitive to the applied power.

V. CONCLUSION

We have measured a large number of planar on-chip resonators and shown that their properties at $T < 1$ K can be understood by using a simple model where the electric field in the resonator is assumed to couple to the bath of two-level fluctuators via dipole interaction. Whilst the presence of TLF is known to affect resonators it is nevertheless quite surprising how well the data can be fitted using a single parameter that is independent of both the frequency over a range of several GHz and the location on the chip. Hence, while our data do not give us a reliable way to identify the nature of these TLF, one can with some certainty conclude that their origin must somehow be intrinsic to the materials used. The bath of TLF appears to have a very wide distribution of both the tunnel splittings and the symmetry parameter of the (effective) double-well. The large nd^2 factor in SiO_2/Si -consistent with previous measurements (see e.g. O'Connell *et al*¹⁵) comes as no surprise given the large density of TLF one would expect in such an amorphous oxide material. The nd^2 factor in sapphire is significantly smaller, but still measurable. This is in itself quite interesting as it is well known that the only two-levels systems seen in very high-quality dielectric sapphire resonators are known to be due to -relatively narrow- electron spin resonances on incidental paramagnetic ions, such as Fe or Cr; if these were the origin of the TLF in our samples one would not expect the data to agree the theory used here. This suggests that the TLF seen here are located in the interface between the film and the substrate, as opposed to the bulk material.

Acknowledgments

We wish to acknowledge Mark Oxborrow, John Gallop, Phil Meeson, Gregoire Ithier, Giovanna Tancredi, Olga Kazakova, Phil Mausskopf and members of NTT Basic Research Laboratories for helpful discussions and comments. This work was supported by EPSRC and the NMI.

* Electronic address: tobias.lindstrom@npl.co.uk

† Also at National Physical Laboratory, Hampton Road, Teddington, TW11 0LW, UK

¹ J. Gao, J. Zmuidzinas, B. Mazin, H. LeDuc, and P. Day, Applied Physics Letters **90**, 102507 (2007).

² S. Kumar, J. Gao, J. Zmuidzinas, B. Mazin, H. LeDuc, and P. Day, Applied Physics Letters **92**, 123503 (2008).

³ R. Barends, H. L. Hortensius, T. Zijlstra, J. J. A. Baselmans, S. J. C. Yates, J. R. Gao, and T. M. Klapwijk, Applied Physics Letters **92**, 223502 (2008).

⁴ A. Wallraff, D. Schuster, A. Blais, L. Frunzio, R. Huang, J. Majer, S. Kumar, S. Girvin, and R. Schoelkopf, Nature **431**, 162 (2004).

⁵ J. Clarke and F. K. Wilhelm, Nature **453**, 1031 (2008).

⁶ L. Faoro, A. Kitaev, and L. B. Ioffe, Physical Review Letters **101**, 247002 (2008).

- ⁷ J. E. Healey, T. Lindstrom, M. S. Colclough, C. M. Muirhead, and A. Y. Tzalenchuk, *Applied Physics Letters* **93**, 3 (2008).
- ⁸ D. Mattis and J. Bardeen, *Physical Review* **111**, 412 (1958).
- ⁹ S. Doyle, P. Mauskopf, J. Naylor, A. Porch, and C. Duncombe, *J. Low Temperature Physics*. pp. 530–536 (2008).
- ¹⁰ C. Song, T. W. Heitmann, M. P. DeFeo, K. Yu, R. McDermott, M. Neeley, J. M. Martinis, and B. L. T. Plourde, [arXiv.org:0812.3645](https://arxiv.org/abs/0812.3645) (2008).
- ¹¹ W. A. Phillips, *Rep. Prog. Phys* **50**, 1657 (1987).
- ¹² U. Strom, M. von Schickfus, and S. Hunklinger, *Physical Review Letters* **41**, 910 (1978).
- ¹³ M. von Schickfus and S. Hunklinger, *Physics Letters* **64A**, 144 (1977).
- ¹⁴ J. Gao, M. Daal, A. Vayonakis, S. Kumar, J. Zmuidzinas, B. Sadoulet, B. A. Mazin, P. K. Day, and H. G. Leduc, *Applied Physics Letters* **92**, 152505 (pages 3) (2008).
- ¹⁵ A. O’Connell, M. Ansmann, R. Bialczak, M. Hofheinz, N. Katz, E. Lucero, C. McKenney, M. Neeley, H. Wang, and E. Weig, *Applied Physics Letters* **92**, 112903 (2008).